









Heterotrophy, microbiome, and location effects on restoration efficacy of the threatened coral *Acropora palmata*

Leila Chapron ^{1✉}, Ilsa B. Kuffner ², Dustin W. Kemp ³, Ann M. Hulver ¹, Elise F. Keister ³, Anastasios Stathakopoulos², Lucy A. Bartlett ², Erin O. Lyons ² & Andréa G. Grottoli ^{1✉}

The iconic and threatened Caribbean coral, *Acropora palmata*, is an essential reef-ecosystem engineer. Understanding the processes underpinning this coral's survival and growth is essential to restoring this foundational species. Here, we compared replicate *A. palmata* colonies transplanted along 350 km of Florida's offshore coral reef to determine holobiont and/or environmental variables that predict transplant success. We found a west-to-east gradient in coral physiology coupled with site-specific coral-associated microbiomes. Interestingly, no variables were linked to coral genet. Our results suggest that the unique oceanographic conditions with periodic upwelling events in the Dry Tortugas provide corals with greater opportunity for heterotrophy that in turn enhances coral growth and survivorship, and positively influences the microbiome. Our findings indicate that restoration efforts in the Dry Tortugas, and other places exhibiting higher food availability, could be most effective for *A. palmata*.

¹School of Earth Sciences, The Ohio State University, 125 S. Oval Mall, Columbus, OH 43214, USA. ²U.S. Geological Survey, St. Petersburg Coastal and Marine Science Center, 600 4th Street South, St. Petersburg, FL 33701, USA. ³Department of Biology, University of Alabama at Birmingham, 1720 2nd Avenue South, Birmingham, AL 35294, USA. ✉email: lchapron@hotmail.fr; grottoli.1@osu.edu

Populations of the elkhorn coral, *Acropora palmata*, have dramatically declined throughout the Caribbean over the past 30 years^{1,2}, leading to its listing as threatened under the United States Endangered Species Act², and as critically endangered by the International Union for Conservation of Nature (IUCN)³. The massive losses in the 1970s and continued decline ever since⁴ are particularly concerning as this species was among the most dominant reef builders for the past 500,000 years throughout the Caribbean⁵. Importantly, *A. palmata* is the primary ecosystem engineer creating reef crest habitat in the western Atlantic that is responsible for coastal protection and economic stability through fisheries and tourism^{6,7}. Thus, conservation and restoration considerations for this species are likely necessary to mitigate the loss of important ecosystem services^{8,9}.

While *A. palmata* is well adapted to persist through some disturbance events such as hurricanes^{2,10}, the region-wide decline has resulted from climate change^{11–13} and the prevalence of marine diseases^{14,15}. Consequences of climate change include heat-stress events that induce coral bleaching, a phenomenon that results from the breakdown of the coral-algal symbiosis. Coral bleaching is the loss of endosymbiotic algae, algal pigmentation, or both, revealing the white skeleton through the colorless host tissue, and giving the coral a pale or white appearance^{16,17}. As endosymbiotic algae facilitate calcification and support metabolism¹⁸, bleached corals suffer losses in energy reserves, decreases in calcification, are more susceptible to disease, and consequently may die^{16,19,20}. After the near loss of *A. palmata* across the Caribbean in the 1980s because of white-band disease¹, recovery of this species can no longer be achieved from natural asexual fragmentation alone, and is now largely dependent upon sexual reproduction and larval recruitment. Successful sexual recruitment of *A. palmata* has rarely been documented throughout the western Atlantic, raising concerns that these populations may be unable to sexually reproduce in many areas of the region^{11–13,21}. The coordination of science, management, and restoration plans could enable the best opportunity to avoid irreversible loss of *A. palmata*^{22,23}.

For example, *Acropora palmata* on the Florida Keys reef tract is often represented by a single or few genets at most sites where it is extant^{21,24}. Recently, an assisted-migration study²³ demonstrated that *A. palmata* may respond positively to genetic rescue, especially at the western terminus of the reef tract in Dry Tortugas National Park (Fig. 1). Genetic clones translocated along the Florida Keys reef tract had greater survival and growth rates in the Dry Tortugas compared to clone mates transplanted to sites in the upper Florida Keys²³. Our follow-up study aimed to determine the factors that may account for this pattern. We postulate that documented periodic upwelling created by cyclonic eddies in the Dry Tortugas^{25–27} could be stimulating primary production and zooplankton, and that this increased food availability might explain the enhanced coral performance. Zooplankton is a key source of nutrition, especially in stressed corals as it is essential for lipid synthesis, tissue growth, and survivorship^{16,18,20,28}. Second, because of the Dry Tortugas' unique and remote location, we suspect that the coral microbiome could differ there compared to the main Florida reef tract. The coral microbiome has been associated with coral health and resilience^{29,30} and may have a probiotic effect in a coral's ability to fight diseases and withstand stress³¹. In some coral species, environmental conditions are known to influence the coral-associated microbial community³². Thus, coral heterotrophy and/or the coral-associated microbiome may be mechanisms underlying the higher growth rates and survivorship of *A. palmata* in the Dry Tortugas compared to other sites in the Florida reef tract²³.

Here, we sampled the surviving corals from Kuffner et al.²³ to test the hypotheses that greater growth and survivorship of *A. palmata* observed in the Dry Tortugas compared to sites in the Florida Keys resulted from (1) higher heterotrophic contributions to their tissues, and/or (2) a shift in the coral-associated microbial community composition, and/or (3) oceanographic conditions. To address the hypotheses, we measured a suite of physiological traits (i.e., survival, biomass, total lipids, total proteins, endosymbiotic density, chlorophyll *a*, $\delta^{13}\text{C}_{\text{h-e}}$, and $\delta^{15}\text{N}_{\text{h-e}}$, wax esters, triacylglycerols, sterols, acetone mobile polar lipids, and phospholipids) and the microbiome community composition (16S rRNA) on replicate colonies of *A. palmata* that were transplanted to five sites along 350 km of offshore reef (6–10 km from land) along the Florida reef tract and the Dry Tortugas, U.S.A.

Healthy corals are associated with high levels of one or more of the following traits: biomass, energy reserves (e.g., total lipids, total protein), endosymbiotic algal density, photosynthesis rates, heterotrophic capacity, and calcification^{17,20,33}. Corals with lower energy reserves and heterotrophic capacity tend to be less resistant to bleaching and recover more slowly from bleaching^{20,33}. In this study, the contribution of heterotrophy to corals tissues was assessed by measuring isotopic proxies ($\delta^{13}\text{C}_{\text{h-e}}$, $\delta^{15}\text{N}_{\text{h-e}}$) and sterols. Lower $\delta^{13}\text{C}_{\text{h-e}}$ and higher $\delta^{15}\text{N}_{\text{h-e}}$ are associated with higher levels of heterotrophy^{32,34}. Sterols are a class of lipids that are derived through diet and increase as coral heterotrophy increases^{35,36}. We measured additional lipid classes: wax esters and triacylglycerols that are storage lipids and tend to be higher in resilient corals, and phospholipids that are the primary component of cellular membranes and tend to decline in bleached corals due to cellular apoptosis^{37,38}. Healthy corals are also strongly dependent on their specific associated microbial communities, as some bacterial taxa play an important role in host nutrition and health^{39,40}. Disturbance of the associated bacteria can lead to the appearance of opportunistic and/or pathogenic microbes, leading to coral disease^{14,15,39}.

By measuring all of these physiological and microbial variables, we provided a wholistic assessment of coral health status along this longitudinal transect. We additionally evaluated the potential influence of environmental conditions on the coral holobiont response. A clearer understanding of what drives the higher growth and survivorship of *A. palmata* in the Dry Tortugas^{23,41,42} could enhance the efficacy of restoration plans for this species throughout the western Atlantic⁴³.

Results

Environmental parameters. In situ seawater temperatures followed similar patterns at each site, with seasonal cycles in temperature ranging from 29 to 32 °C in summer and from 22 to 25 °C in winter (Supplementary Fig. 1 and Kuffner et al.⁴⁴). During the experimental period, temperature exceeded the bleaching threshold for only short interludes (i.e., few days) and, expressed in degree heating weeks, did not vary significantly among sites (Supplementary Fig. 1 and Kuffner et al.²³). Between November 2019 and March 2020, seawater temperature was at times up to 2 °C colder at both Pulaski West and Pulaski Light in the Dry Tortugas compared to the Florida Keys sites, suggesting upwelling events. Wind speed exhibited similar temporal variability among sites (Supplementary Fig. 2). Total bulk zooplankton concentrations were highest at Pulaski West (2159 ± 369 zooplankton L^{-1}) and lowest at Sombrero Reef (962 ± 161 zooplankton L^{-1}) (Supplementary Fig. 3). More than 14 functional groups of zooplankton were identified, and samples from all sites were dominated by copepods, which were most abundant at Pulaski West (1458 ± 339 zooplankton L^{-1}).

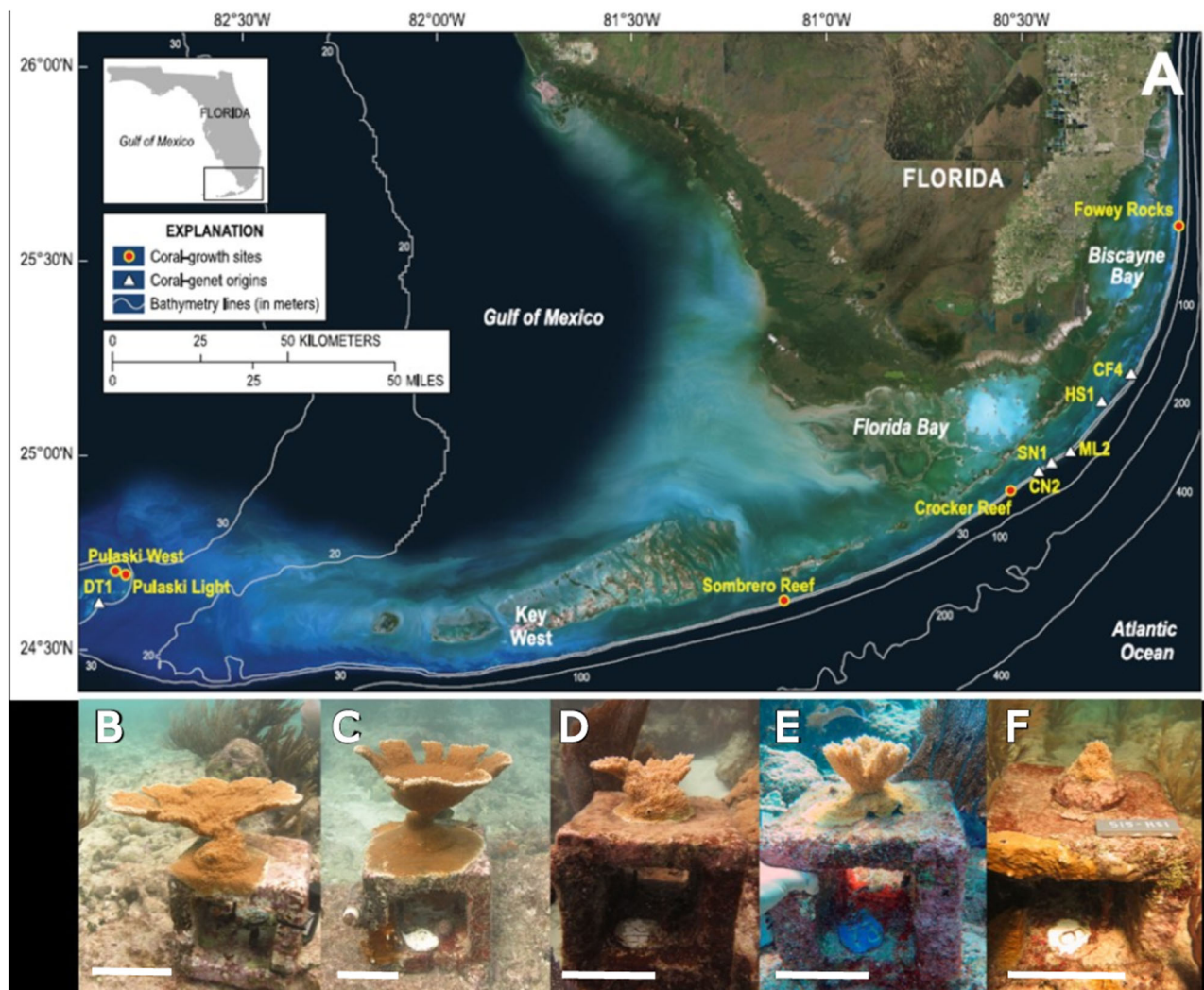


Fig. 1 Map of collection sites, study sites, and examples of corals at each study site. **A** Map showing the original collection sites (white triangles) of genets CF4, CN2, HS1, ML2, and SN1 prior to placement in the Coral Restoration Foundation offshore nurseries, and of genet DT1 in the Coral Species Protection Zone in Dry Tortugas National Park, and study sites (red circles) where nursery-raised fragments of those genets were transplanted to experimental blocks on the offshore reef (6–10 km from the shore). Genet-collection site abbreviations are DT1 Dry Tortugas, CN2 Conch Reef, SN1 Snapper Ledge, ML2 Molasses Reef, HS1 Horseshoe Reef, and CF4 Carysfort Reef. Figure adapted from Kuffner et al.(2020)¹⁹. Shown in the lower panels are examples of coral ramets that grew at least 2 years at **(B)** Pulaski West (24.70° N, 82.80° W), **(C)** Pulaski Light (24.69° N, 82.77° W), **(D)** Sombrero Reef (24.63° N, 81.11° W), **(E)** Crocker Reef (24.91° N, 80.53° W), and **(F)** Fowey Rocks (25.59° N, 80.10° W). Scale bars represent 10 cm. Photos by USGS, and base map is uncopyrighted from World_Imagery; source: Esri, DigitalGlobe, GeoEye, Earthstar Geographics, CNES/Airbus DS, USGDA, USGS, AES, Getmapping, Aerogrid, IGN, IGP, Swisstopo, and the GIS user community.

Survival. In situ seawater temperature exceeded the bleaching threshold for brief amounts of time (i.e., days) during the late summer of 2018, 2019, and 2020 at all sites²³ (Supplementary Fig. 1). Since the corals were not monitored during the peak bleaching season, it is unknown if bleaching of the experimental corals occurred during the study. During the Autumn 2020 sampling, 100% of the ramets at both Dry Tortugas sites were alive, though 4 of the 24 had too little live tissue remaining to sample for downstream laboratory analyses (Supplementary Table 1). Complete mortality rates at the Florida Keys sites were 70%, 20%, and 50% at Sombrero Reef, Crocker Reef, and Fowey Rocks, respectively (Supplementary Table 1). A total of 41 corals were alive and available for sampling in this study (Supplementary Table 1).

Physiological profile among sites. The overall physiological profile of *A. palmata* significantly differed among all sites except

between Sombrero Reef and Crocker Reef (Fig. 2a, Supplementary Table 2). A strong west-to-east pattern was observed in all physiological variables except for the difference between $\delta^{13}\text{C}$ of the host and algal endosymbionts ($\delta^{13}\text{C}_{\text{h-e}}$, Fig. 2a, Supplementary Table 3). Closer examination revealed that total lipids, total proteins, endosymbiont density, and chlorophyll *a* gradually decreased from west to east (Fig. 2c–f, Supplementary Table 4), whereas biomass gradually increased from west to east (Fig. 2b, Supplementary Table 4). Finally, *A. palmata* exhibited the lowest $\delta^{13}\text{C}_{\text{h-e}}$ in the Dry Tortugas (Pulaski West and Pulaski Light) and at Fowey Rocks (Fig. 2g, Supplementary Table 4).

Lipid-class profiles among sites. The overall lipid-class profiles of *A. palmata* significantly differed among sites in the Florida Keys, but not among the Pulaski West, Pulaski Light, and Sombrero Reef sites (Fig. 3a, Supplementary Table 5). The west to east pattern was driven mostly by the sterols, phospholipids, and wax

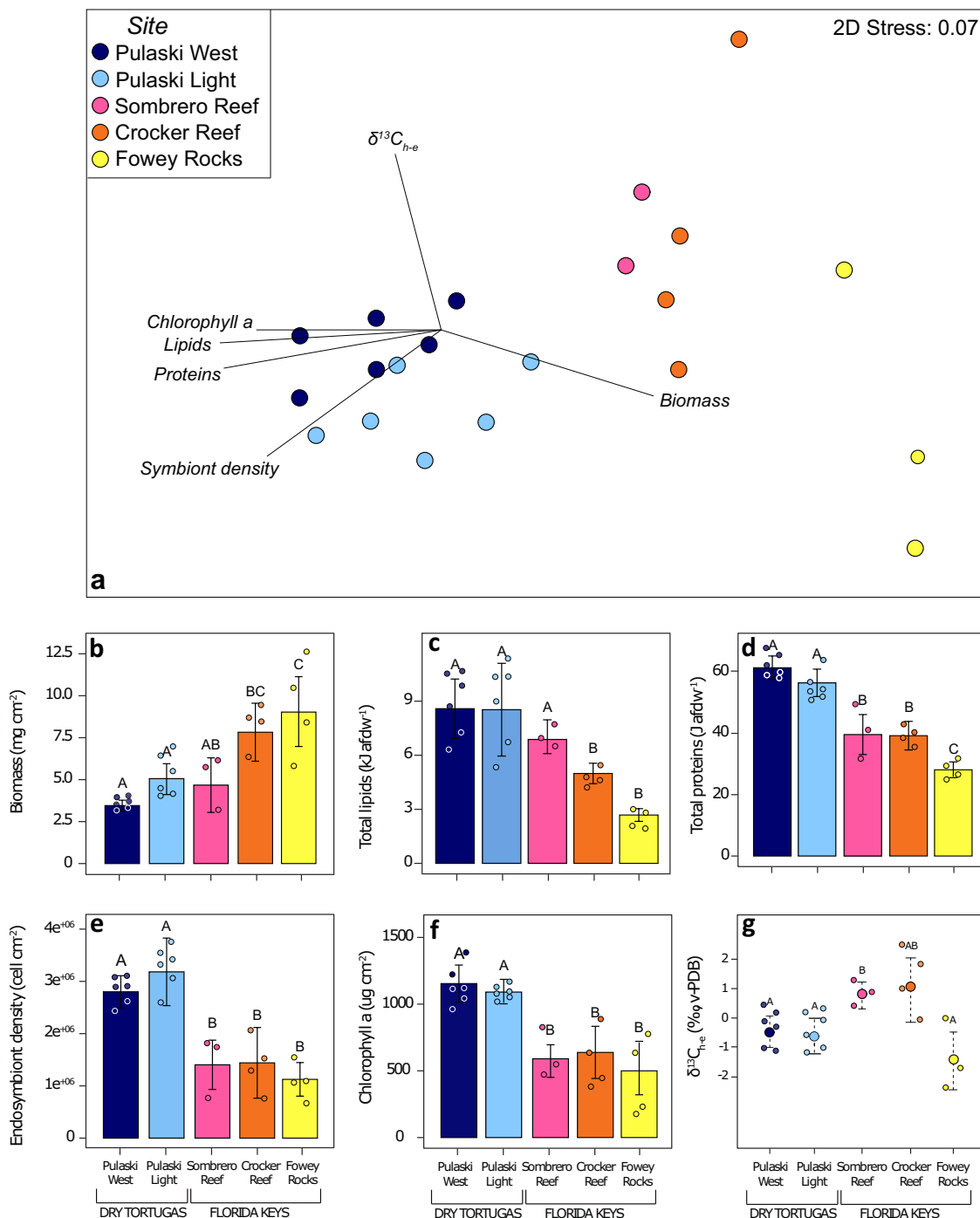


Fig. 2 Coral physiology at each study site. **a** Multivariate NMDS plot ($R = 0.7$) for physiological profiles of *Acropora palmata* from Pulaski West (dark blue), Pulaski Light (light blue), Sombrero Reef (magenta), Crocker Reef (orange), and Fowey Rocks (yellow). Vectors indicate strength and direction of the relative contribution of each physiological trait to the sample distribution as determined by Pearson's correlation analysis. Corresponding ANOSIMs results are in Supplementary Table 2. **b–g** Average (± 1 standard error) biomass, total lipids, total proteins, endosymbiont density, chlorophyll *a*, and $\delta^{13}\text{C}_{\text{h-e}}$ (coral carbon isotopic difference between host and endosymbiont) of *A. palmata* at each site. All corresponding Kruskal-Wallis, ANOVA, and Tukey post hoc results are in Supplementary Table 4.

esters (Fig. 3a, Supplementary Table 6). Closer examination revealed that these three lipid classes were the highest in the Dry Tortugas (Pulaski West and Pulaski Light) corals, and gradually decreased from west to east (Fig. 3b, d, f, Supplementary Table 7). In contrast, triacylglycerols and acetone-mobile polar lipids values did not significantly differ among sites (Fig. 3c, e, Supplementary Table 7).

Coral bacterial community. The seawater bacterial communities were similar among sites but did differ from coral-associated bacterial communities (Fig. 4a; Supplementary Table 8). Further, the coral-associated bacterial community compositions differed among sites (Fig. 4a, Supplementary Fig. 4, Supplementary Table 8), except between Pulaski Light and Sombrero Reef, and between Crocker Reef and Fowey Rocks. The coral-associated

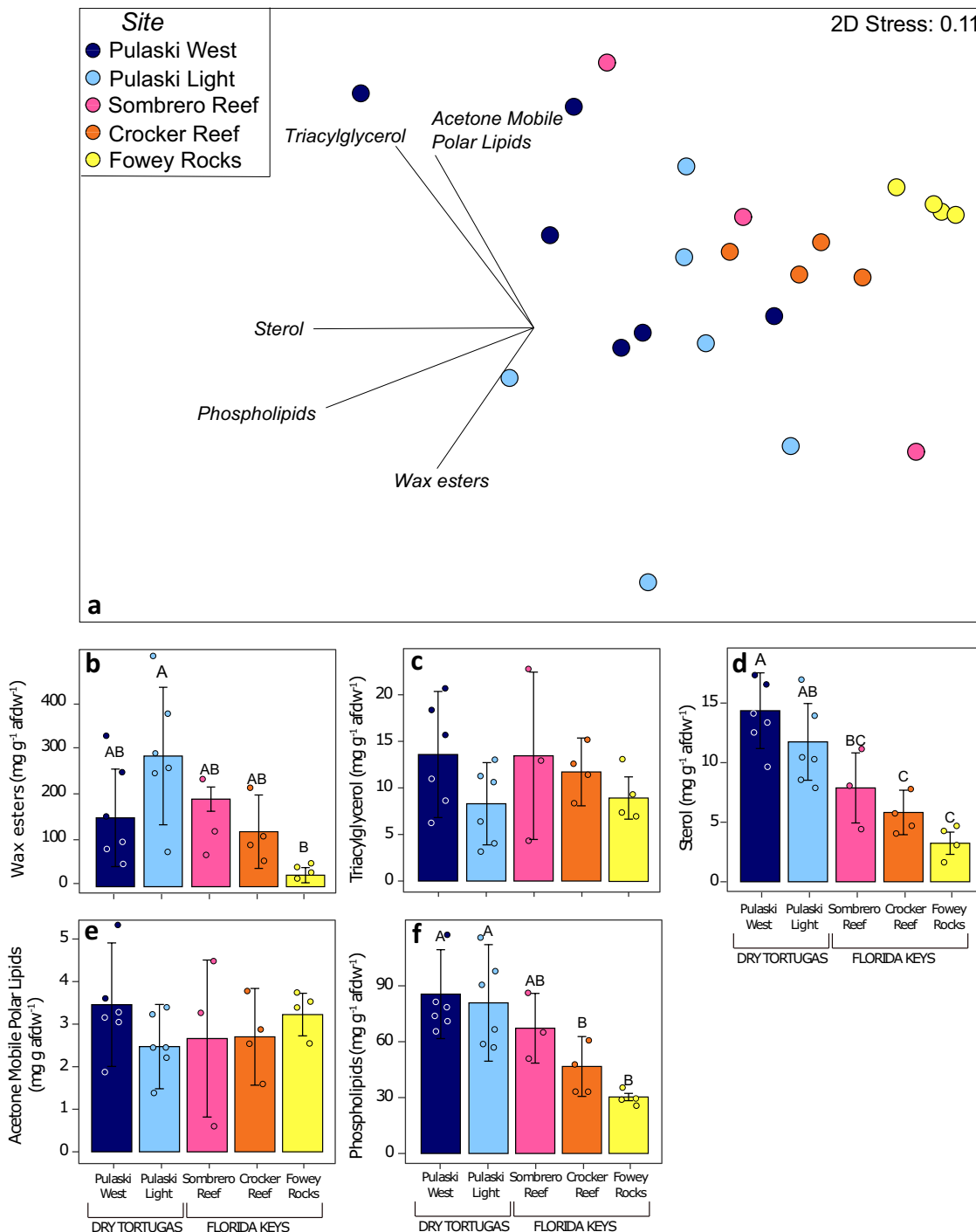


Fig. 3 Coral lipid classes at each study site. **a** Multivariate non-metric multidimensional scaling (NMDS) plot ($R = 0.4$) using lipid class composition values of *Acropora palmata* from Pulaski West (dark blue), Pulaski Light (light blue), Sombrero Reef (magenta), Crocker Reef (orange), and Fowey Rocks (yellow). Vectors indicate strength and direction of the relative contribution of each lipid class to the sample distribution as determined by Pearson’s correlation analysis. Corresponding ANOSIMs results are in Supplementary Table 5. **(b–f)** Average proportion (± 1 standard error) of wax esters, triacylglycerol, sterol, acetone mobile polar lipids, and phospholipids relative to ash free dry weight of *A. palmata* at each site. All Kruskal-Wallis, ANOVA, and Tukey post hoc results are in Supplementary Table 7.

bacterial communities showed the highest Shannon diversity in *A. palmata* from Pulaski Light and Sombrero Reef (Fig. 4b). At the class level, the *A. palmata* bacterial communities were mostly dominated by *Alphaproteobacteria* (~24%), *Gammaproteobacteria* (~18%), and *Spirochaetia* (~17%) (Supplementary Fig. 4). Higher proportions of *Spirochaetia* coupled to lower proportions of *Cyanobacteria* were observed in Pulaski West corals compared

to corals at all other sites (Supplementary Fig. 4). The proportional abundance of the class *Deinococci* was higher in Crocker Reef and Fowey Rocks corals compared to the other sites (Supplementary Fig. 4). At the amplicon sequence variant (ASV) level, the ASV1, ASV2, ASV3, ASV4, ASV5, ASV6, ASV7, ASV31 and ASV39 contributed proportionately the most to the differences in coral microbiomes among sites (Fig. 4c–k, Supplementary

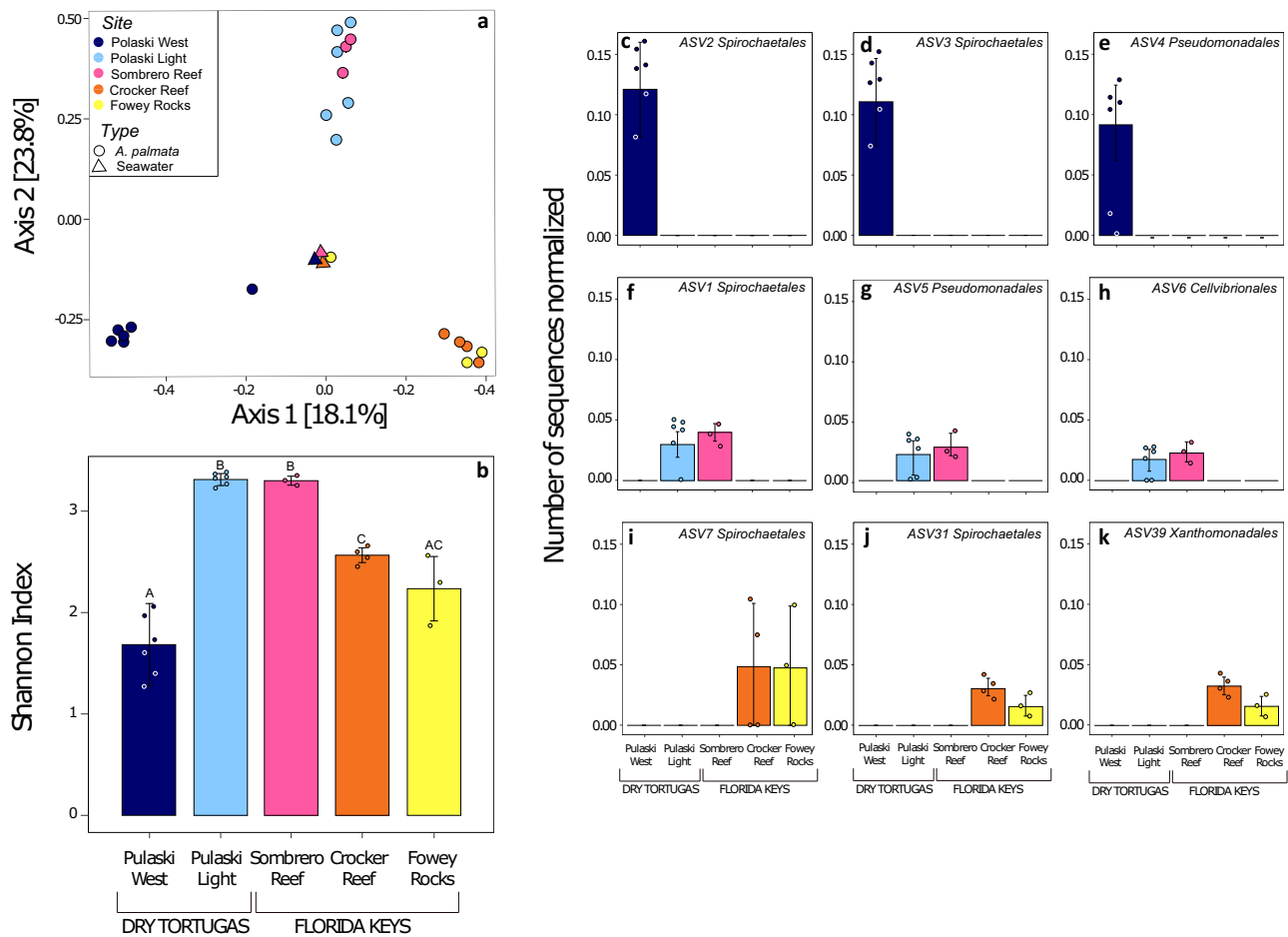


Fig. 4 Coral and seawater microbiomes at each study site. **a** Non-multi-dimensional scaling plot (NMDS) showing the similarity between bacterial community compositions for *Acropora palmata* (circles) and seawater (triangles) from Pulaski West (dark blue), Pulaski Light (light blue), Sombrero Reef (magenta), Crocker Reef (orange), and Fowey Rocks (yellow). Bacterial communities are described based on the 16 S rRNA gene. **b** Average (± 1 standard error) Shannon diversity index of *Acropora palmata* at each site. Averages with the same letter do not differ from each other based on one-way ANOVA analysis (Kruskal-Wallis chi squared = 2.7, $df = 4$, p -value < 0.01). **c–k** Average (± 1 standard error) relative abundance of the ASVs (amplicon sequence variants) that contributed proportionally the most to the differences in coral-associated microbial communities among sites as determined by SIMPER analysis. Detailed taxonomic affiliation of the selected ASVs are in Supplementary Table 9.

Table 9). The ASV2 (order *Spirochaetales*), ASV3 (*Spirochaetales*), and ASV4 (*Pseudomonadales*) were found exclusively in *A. palmata* from Pulaski West and represent 12, 11 and 9% respectively of the total relative abundance (Fig. 4c–e, Supplementary Fig. 4). The ASV1 (*Spirochaetales*), ASV5 (*Pseudomonadales*), and the ASV6 (*Cellvibrionales*) were only found in *A. palmata* from Pulaski Light and Sombrero Reef (Fig. 4f–h). Finally, the ASV7 (*Spirochaetales*), ASV31 (*Spirochaetales*), and ASV39 (*Xanthomonadales*) were found only in *A. palmata* from Crocker Reef and Fowey Rocks (Fig. 4i–k). ASV37 (*Campylobacteriales*) was found exclusively in *A. palmata* from Fowey Rocks (Supplementary Fig. 5, Supplementary Table 9). Detailed taxonomic affiliation of the identified ASVs are in Supplementary Table 9. Finally, no physiological variables significantly described the overall microbiome NMDS distribution for *A. palmata* (BEST, $R = 0.18$, $p = 0.76$).

Discussion

Our findings suggest that enhanced feeding opportunity and favorable coral-associated microbiomes supported higher survivorship and growth of *Acropora palmata* transplanted to the Dry Tortugas compared to corals moved to sites in the Florida

Keys, independent of coral genet²³. The unique oceanographic conditions in the Dry Tortugas that produce periodic upwelling most likely enhanced coral-feeding opportunities⁴⁵ and specific coral microbial community composition^{46,47}. Here, we present multiple lines of evidence to support this conclusion.

Elevated heterotrophy is associated with coral resilience as feeding can provide a critical source of fixed carbon to bleached and recovering corals, allowing them to meet metabolic demand, build tissue, and synthesize lipid thereby reducing the probability of mortality from heat-stress^{16,20,28,48}. When corals are deprived of zooplankton, their calcification rates, survivorship, and other health indicators decline^{49–51}.

Here, the overall physiology of the transplanted *A. palmata* colonies in the Dry Tortugas was distinct from those transplanted to the middle and upper Florida Keys sites (Figs. 2a, 3a). Four lines of evidence suggest that heterotrophy played an important role in the observed coral performance²³ (Fig. 2). First, lipids and proteins that provide stored energy for sustaining corals^{20,52} were higher in *A. palmata* from the western sites compared to the eastern sites (Fig. 2c, d). Higher levels of energy reserves in corals are associated with high basal-feeding rates and/or high heterotrophic plasticity^{20,33,53}. Corals with higher lipid and/or protein concentrations are more likely to survive heat-stress events,

acidification, and smothering by sedimentation^{17,33,54}, and have higher calcification rates⁵¹. The lower biomass observed in the Dry Tortugas corals is most likely a function of the much faster skeletal growth, resulting in a thinner tissue layer and biomass per unit area (Fig. 2b). Second, endosymbiotic algal density and chlorophyll *a* were higher in the Dry Tortugas corals compared to the main Florida reef tract corals (Fig. 2e, f), despite corals all being at similar depths. Since chlorophyll *a* or coral pigmentation increases as feeding rates increase in Hawaiian corals⁵⁵, these physiological traits in *A. palmata* may be higher due to increased heterotrophy^{50,51,55}. Thus, it is unlikely that the site differences we observed were driven by differences in light availability, as chlorophyll *a* did not differ between the two Dry Tortugas sites (Fig. 2f), even with the Pulaski Light site being slightly deeper (4–6 m at Pulaski Light vs 4–5 m at Pulaski West). Third, sterols and phospholipids decreased from west to east with higher values in the Dry Tortugas corals (Fig. 3d–f). Sterols in corals are primarily derived heterotrophically and their abundance in corals is a strong indicator of heterotrophy^{35,36}, while phospholipids are the primary component of cellular membranes^{37,38}. The elevated coral sterols and phospholipids in the western sites suggest higher levels of heterotrophy and higher tissue growth, respectively. Fourth, the $\delta^{13}\text{C}_{\text{h-e}}$ values show that the proportionate contribution of heterotrophically derived versus photoautotrophically derived carbon was significantly greater at the Dry Tortugas sites compared to the Sombrero Reef corals, but not Fowey Rocks corals (Fig. 2g). Overall, the higher energy reserves, endosymbiotic algal density, chlorophyll *a*, sterols, and phospholipids, and to a lesser extent the lower $\delta^{13}\text{C}_{\text{h-e}}$ values, strongly support the hypothesis that the higher survivorship and growth of *A. palmata* ramets in the Dry Tortugas compared to the main Florida Keys sites²³ (Supplementary Table 1) were due to higher heterotrophy.

Coral bacterial communities are involved in key coral-physiological functions such as immune response and nutrient acquisition, and thus appear to play a role in holobiont resilience^{30,39,40}. The coral microbial diversity and community composition of our corals differed among sites (Fig. 4a, b). The ASVs most responsible for differences in microbial community composition of *A. palmata* across sites were unique at each site (Fig. 4c–k) despite there being no difference in the seawater microbial communities among sites (Fig. 4a). The lack of any differences in seawater microbial community composition among sites suggests that the differences in coral-associated microbial communities are dependent on the host coral. While no measured physiological characteristics were strongly correlated with the *A. palmata* microbiome (BEST analysis, Figs. 2, 4), the apparent greater heterotrophy in the Dry Tortugas corals could be a driver of the microbial community composition, as diet has been shown to influence the coral microbiome⁵⁶. As for host-coral genetic effects on the microbiome, our results mirror those of Rosales et al.⁴⁷, who similarly found no influence of the coral genet on the associated microbial communities. Similar to other studies, *Alphaproteobacteria*, *Gammaproteobacteria*, and *Cyanobacteria* were ubiquitous, can have beneficial or harmful properties, and are usually the most represented bacterial classes in corals^{29,57–59}, including *A. palmata*^{60,61}. *Spirochaetia*, which were dominant in all our *A. palmata* samples and were present in similar relative abundance as in other studies^{47,61}, are common to both healthy and stressed corals⁵⁹ and are implicated in nitrogen fixation⁶². *Deinococci*, which were found in our corals at the eastern-most site, has been observed in thermally stressed *Acropora* species suggesting a potential role of this taxa in holobiont stress response⁶³. The bacterial orders *Pseudomonadales* and *Cellvibrionales* (containing the family *Cellvibrionaceae*), which were abundant in the Dry Tortugas and Sombrero Reef corals (Fig. 4e, g, h), are associated with essential

roles such as nutrition, antifouling, and antibacterial activity, especially in oligotrophic environments^{64,65}. The order *Xanthomonadales*, shown to be associated with ocean-acidification stress responses in *Isopora palifera* and *Porites lobata*⁶⁶, was found in higher abundance at the easternmost sites of Fowey Rocks and Crocker Reef (Fig. 4k), suggesting that these sites may be stressful for *A. palmata*. Finally, corals at Fowey Rocks contained the order *Campylobacterales* (ASV37, Supplementary Fig. 5), which is known to be associated with coral diseases such as black-band disease, white syndrome, brown-band disease, and white plague⁵⁷. Thus, the differences in bacterial communities we observed suggest that the holobiont environment supports favorable to less-favorable coral-associated microbial communities along a west-to-east gradient on the Florida reef tract.

The noticeable transition in coral survivorship, growth, physiology, and coral-associated bacterial communities that we observed in corals transplanted along the Florida reef tract, from west to east, could be driven by one or more of the following oceanographic factors: (1) differences in zooplankton abundance, diversity, and/or nutritional quality from west to east (Supplementary Fig. 3) and/or (2) periodic, cooler temperatures in non-summer months in the Dry Tortugas compared to the Florida Keys (Supplementary Fig. 1), and/or (3) water quality factors (e.g., inorganic nutrients).

Based on a single night of sampling at each site, there was evidence of higher total zooplankton abundance and copepod abundance in the Dry Tortugas compared to the other sites (Supplementary Fig. 3). Corals do feed more as zooplankton concentrations increase^{51,55,67} and copepods can constitute up to 50% of the zooplankton captured by Caribbean corals^{68,69}. However, additional sampling over the course of the year would be needed to verify if zooplankton abundance systematically differs across our sites and/or seasonally. Nevertheless, it is reasonable to hypothesize that zooplankton abundance would be at least periodically higher in the Dry Tortugas, as this site experiences complex oceanographic dynamics, with the Loop Current and Tortugas gyres bringing periodic upwelling that delivers cooler, nutrient-rich seawater to the surface^{25,26,70} (Supplementary Fig. 1), which in turn stimulates primary production and zooplankton concentrations^{71,72}. Hydrologic features in the Dry Tortugas also contribute to eddy transformations that can produce upwelling⁷⁰. Thus, the specific oceanographic setting of the Dry Tortugas suggests that zooplankton concentrations and/or composition could be systematically, or periodically, different there than along the main Florida reef tract⁷³. This is consistent with our isotope and sterol data that suggest greater heterotrophy in Dry Tortugas corals.

In addition, cool upwelled seawater could benefit corals by limiting thermal stress^{71,74}. However, in situ seawater temperature monitored during our study at the different sites showed that upwelling events in the Dry Tortugas did not occur in the summer months, when temperatures are the most stressful for corals (Supplementary Fig. 1⁴⁴). Tortugas gyres are produced by the dynamic behavior of the Loop current, but their timing does not display regular seasonality^{25,26}. Thus, periodic trophic-web stimulation via input of nutrients from oceanographically driven upwelling in the Dry Tortugas is a plausible, influential driver of the higher *A. palmata* survivorship and growth. Differences in ocean dynamics on small and larger scales can influence the spatial population structures of corals and may prove critical for future coral survivorship during moderate increases in seawater temperatures⁷⁵.

Finally, long-term monitoring of water quality indicators (e.g., nutrient concentrations) suggests that there are no sustained anthropogenically driven differences in water quality between the Dry Tortugas and the offshore Florida Reef Keys reefs where our sites were located (6 to 10 km from land)^{76–78}. However, periodic

upwelling in the Dry Tortugas²⁷ could provide pulses of moderate levels of nutrients that would stimulate primary and secondary production (i.e., phytoplankton and zooplankton blooms), which could support more heterotrophic opportunities for corals. Oceanographic dynamics and diet can also shape the coral-associated bacterial communities, as they are involved in the cycling of key elements such as carbon and nitrogen⁵⁶. Thus, periodic upwelling may lead to more heterotrophy and a more versatile coral microbiome conducive to higher coral fitness and growth^{46,47}.

The fourteen ramets that died at the main Florida Keys sites, were from all five of the coral genets (Supplementary Table 1), and mortality was not statistically associated with coral genet²³. Additionally, there were no significant coral-genet effects detected for any of the coral physiological variables, lipid classes, or microbial community compositions (Supplementary Tables 10, 11, 12), suggesting that environment was a larger driver of coral health than genotype. This is consistent with observations of enhanced growth and reproductive capacity of *Porites astreoides* colonies in the Dry Tortugas compared to colonies in the Florida Keys⁴², but contrary to past studies showing significant influences of genet on the coral physiology and microbiome^{79–81}. As our study was conducted with only five coral genets sourced from the same nursery, additional research on *A. palmata* that includes greater genotypic diversity is needed to confirm our findings.

In summary, our results clearly show that *Acropora palmata* corals transplanted to the Dry Tortugas were thriving compared to their genetic clones translocated to the main Florida Keys sites. Interestingly, a recent study showed this was also the case for natural *A. palmata* populations along the Florida reef tract, with the highest amount of live coral tissue being reported in Dry Tortugas National Park⁸². Our corals translocated to the Dry Tortugas had the highest growth rates²³, suffered no complete mortality (Supplementary Table 1), and simultaneously contained the highest concentrations of lipids, sterols, proteins, endosymbiotic algae, and chlorophyll *a*, while also having distinct microbial communities compared to the other sites (Figs. 2, 3 & Supplementary Fig. 4). The oceanographic conditions that drive periodic upwelling in the Dry Tortugas, coupled with our coral physiology data and limited zooplankton data, provide evidence that the most likely reason for the greater physiological health and performance of *A. palmata* in the Dry Tortugas is increased access to heterotrophic food resources. Together, our findings are consistent with the hypothesis that the oceanographic conditions in the Dry Tortugas are, at least in today's ocean, better suited for the extant genetic strains of *A. palmata* we tested compared to other locations in the main Florida Keys. These findings further solidify the propitious role of the Dry Tortugas for hosting, through restoration, a sexually reproducing, viable population to help this coral species recover regionally²³. The "upstream" location of the Dry Tortugas, with respect to the Florida Current, has the added benefit of being a potential source population of *A. palmata* that could supply larvae to the more degraded Florida Keys reefs⁴².

Materials And methods

To test our first hypothesis that higher growth and survivorship of *A. palmata* in the Dry Tortugas was due to higher heterotrophy, we compared the holobiont physiological profiles (i.e., biomass, total lipids, total proteins, endosymbiont density, chlorophyll *a*, and $\delta^{13}\text{C}_{\text{org}}$) and lipid class profiles (i.e., wax esters, triacylglycerol, sterols, acetone-mobile polar lipids, and phospholipids) in genetically replicated colonies of *A. palmata* that were out-planted along three sites on the Florida Keys outer reef tract (Fowey Rocks, Crocker Reef, Sombbrero Reef) and at two sites in the Dry Tortugas National Park (Pulaski West and Pulaski Light) for at least 25 months using a combination of multivariate and univariate statistics. To test our second hypothesis that higher growth and survivorship of *A. palmata* in the Dry Tortugas was due to the coral microbiome, we compared the coral-associated microbial community composition and diversity of corals from each site, and also compared the seawater microbial community to that of the corals using a combination of multivariate and univariate statistics. To evaluate the last hypothesis that higher growth and survivorship of *A. palmata* in the Dry Tortugas

was due to environmental conditions, we compared the zooplankton concentration and community composition at all sites, as well as the in situ seawater temperature and wind speed. Zooplankton sample size was insufficient to conduct robust statistical analyses. Details of the laboratory and statistical analyses are below, in the Supplemental Materials, and in the metadata of the U.S. Geological Survey data releases associated with this study^{44,83,84}.

Coral collection and experimental design. Details of the experimental design are described in Kuffner et al.²³ and raw data and metadata are available in Kuffner et al.⁸³, and Chapron et al.⁸⁴ Briefly, ramets (5 × 5 × 3 cm) from five genets of *Acropora palmata* (CF4, CN2, HS1, ML2, and SN1) were collected from offshore reefs in the upper Florida Keys by the Coral Restoration Foundation staff and propagated in their offshore coral nurseries for at least two years before being sampled for our experiment. Originally, genet CF4 was from Carysfort Reef (25.37° N, 80.25° W, collected in May 2014), genet CN2 was from Conch Reef (24.78° N, 80.55° W, collected in September 2012), HS1 was from Horseshoe Reef (25.24° N, 80.47° W, collected in August 2014), ML2 was from Molasses Reef (25.17° N, 80.49° W, collected in March 2014) and SN1 was from Snapper Ledge reef (25.21° N, 80.51° W, collected in May 2009) (see white triangles in Fig. 1, and additional information in the Supplemental Materials). A sixth genet, the last known living genet of *A. palmata* in Dry Tortugas National Park at the time of the study, was first acquired as fragments-of-opportunity following storm breakage in the Coral Species Protection Zone south of Garden Key at an unknown time prior to 2016 and then housed in The Nature Conservancy's Garden Key coral nursery until we obtained samples for our experiment in May 2018. This sixth genet was included in the experiment only at the two Dry Tortugas sites, as permitting restrictions did not allow for transplantation of this genet outside of the Dry Tortugas. Ramets were deployed on secured cinderblocks to Pulaski West, Pulaski Light, Sombbrero Reef, Crocker Reef, and Fowey Rocks (Fig. 1) in Spring 2018, and six additional 6 ramets from genets CN2, HS1, and SN1 were deployed at Crocker Reef in Spring 2017. All sites were 6–10 km from land, in similar low-relief offshore-reef habitat, and at a consistent depth of 4–6 m.

The surviving coral ramets and one liter of seawater were collected at the Sombbrero Reef, Crocker Reef, and Fowey Rocks sites on 29–30 October 2020. Collection at the Dry Tortugas sites was delayed to 28–30 November 2020 due to Hurricane Eta. The seawater and collected coral ramets were immediately put on ice following collection. The seawater was filtered onto a sterile 0.22 μm filter after prefiltration through a sterile 3 μm pore-size polycarbonate filter (Millipore Sigma). All coral fragments and filters were frozen at –20 °C, transported to The Ohio State University on dry ice, and then stored at –80 °C until further analysis. Nitrile gloves were worn for all collections and sample handling. Additional coral collection and experimental design details are provided in the Supplemental Materials.

Oceanographic conditions. In situ seawater temperature was recorded from 8 May 2018 to 30 November 2020 using HOBO Water Temp Pro v2 temperature loggers (Onset, Pocasset, MA, USA, ±0.2 °C precision) deployed in duplicate at each site⁴⁴ (Supplementary Fig. 1). Wind speed, which is a proxy for water-column mixing, was extracted from The National Data Buoy Center (Supplementary Fig. 2)⁸⁵. For each site, one bulk zooplankton sample was collected at night on 29, 30 October 2020 for Crocker Reef and Sombbrero Reef, respectively and on 28, 29 November 2020 for Pulaski West and Pulaski Light, respectively. One bulk zooplankton sample was collected at the end of the day (6 pm) on 31 October 2020 for Fowey Rocks because night sampling was not possible due to the complexity accessing this site at night. Due to logistical and travel constraints imposed by Covid-19 pandemic restrictions in the spring, summer, and fall of 2020 that severely limited the number of days of fieldwork, it was not possible to collect additional zooplankton samples. Bulk zooplankton sample collections were performed using a 0.5 m diameter plankton net with 50 μm pore-size mesh towed for 130 (±25) meters at 0.5 m depth below the surface. Each collected bulk-plankton sample was preserved in 10% formalin, and thirty-two 1 mL subsamples of each sample were counted using a dissection microscope. Zooplankton concentrations of each major functional group were calculated per liter of seawater.

Laboratory analyses. Each ramet was cut into three sections along the axis of growth using a sterilized diamond blade tile saw. One section was reserved for physiological analyses (i.e., biomass, endosymbiont density, chlorophyll *a*, lipids with the lipid classes, and proteins), one for isotopic analyses ($\delta^{13}\text{C}_{\text{h}}$, $\delta^{13}\text{C}_{\text{e}}$, $\delta^{15}\text{N}_{\text{h}}$, $\delta^{15}\text{N}_{\text{e}}$), and one for microbial community composition.

The surface area of each ramet section designated for physiological analyses was determined using the aluminum-foil method⁸⁶, then ground to a homogeneous paste (skeleton, host, and endosymbiont) and divided into 5 sub-samples, one for each of the physiological analyses. Tissue biomass was measured using methods described by McLachlan et al. (2020a)⁸⁷. Endosymbiont density was measured using 4 replicated counts on a Countess II FL Automated Cell Counter⁸⁸. Chlorophyll *a* was extracted using a double 100% acetone extraction and quantified with a spectrophotometer using the equation from Jeffrey and Humphrey (1975)⁸⁹. Tissue biomass, endosymbiont density, and chlorophyll *a* were standardized to surface area based on the proportional representation of each of their respective sub-samples.

Total lipids were extracted using a chloroform:methanol solution and proteins were extracted using the Bio-Rad protein assay solution following established methods of McLachlan et al. (2020c)⁹⁰ and Bradford (1976)⁹¹, respectively. The energetic value of total lipid and protein concentrations were reported in joules⁹² and standardized to ash-free dry weight of the coral tissue.

Isotopic analyses were assessed on separated animal host and algal endosymbiont fractions using methods described in Price et al.³² From the ramet section designated for isotopic analyses, between 4 to 8 cm² of coral tissue was removed using an airbrush, and the host and endosymbiont fractions were separated by centrifugation and filtration. Each sample was individually combusted using a PDZ Europa ANCA-GSL element analyzer interfaced to a PDZ Europa 20-20 isotope ratio mass spectrometer (Sercon Ltd., Cheschier, UK) at the University of California Davis Stable Isotope Facility. The carbon and nitrogen isotopic composition of the animal host ($\delta^{13}\text{C}_h$, $\delta^{15}\text{N}_h$) and algal endosymbiont ($\delta^{13}\text{C}_e$, $\delta^{15}\text{N}_e$) were reported as the per mil deviation of the stable isotopes ^{13}C : ^{12}C relative to Vienna-Pee Dee Belemnite Limestone Standard (v-PDB) and ^{15}N : ^{14}N relative to air, respectively. Repeated measurements of internal standards had a standard deviation of $\pm 0.2\text{‰}$ and $\pm 0.23\text{‰}$ for $\delta^{13}\text{C}$ and $\delta^{15}\text{N}$, respectively. The difference between $\delta^{13}\text{C}_h$ and $\delta^{13}\text{C}_e$ ($\delta^{13}\text{C}_{h-e}$) and the $\delta^{15}\text{N}_h$ and $\delta^{15}\text{N}_e$ ($\delta^{15}\text{N}_{h-e}$) both represent the relative contribution of photoautotrophic versus heterotrophic carbon to coral tissues^{32,34,93}.

The total lipids were dried under nitrogen gas over a water bath at 55 °C. The vials containing the dried total lipids were frozen at -80 °C and transported on dry ice to the University of Alabama at Birmingham for lipid class analysis. The dried total lipids were resuspended in 100% chloroform at a concentration of 10 mg mL⁻¹. Lipid class composition was analyzed by an Iatroscan MK 6 S thin layer flame ionization detector (NTS) according to the methods modified from Conlan et al.³⁷ as described in Keister et al.⁹⁴ Briefly, we spotted 1 μL of the solution, in duplicate, onto each thin layer quartz-impregnated rod (Chromarods Mitsubishi Kagaku Iatron, Inc) of the Iatroscan rack using a metal and glass syringe. The rack, containing ten loaded rods were placed in the first closed development chamber containing 50:20:1 (v:v:v) chloroform:methanol:Milli-Q and developed to half height (~7 min). The rack was then dried for 2 min at room temperature and transferred to the second closed development chamber containing 57:14.2:1.4 (v:v:v) hexane:ethyl ether:formic acid and developed to full height (~17 min). The rack of rods was dried in the oven at 100 °C for 10 min prior to being scanned using flame ionization detection with an Iatroscan MK 6 S detector (Air pressure at 2, Hydrogen flow at 165 mL min⁻¹).

The amount of each lipid class (wax esters, triacylglycerol, sterols, acetone mobile polar lipids, and phospholipids) on each rod was determined by comparison to a standard curve produced from 1 μL standards of known concentrations for each lipid class, ranging from 0.078 mg mL⁻¹ to 10 mg mL⁻¹. Each lipid class concentration was normalized to the amount of total lipid initially extracted and standardized to ash-free dry weight for each sample. Each sample was run in duplicate, and the results of the duplicate runs were averaged to produce one lipid class value for each coral ramet sample.

The coral bacterial community for each sample was assessed from coral tissues airbrushed from the ramet section designated for microbial analyses using sterile techniques. Seawater bacterial communities were assessed from the 0.22 μm filters. For DNA extraction, coral tissues and filters were individually homogenized with a TissueLyser LT (Qiagen Inc., Valencia, CA, USA). DNA extractions were performed using the DNeasy PowerSoil Pro Kit (Qiagen, Germantown, MD) following the manufacturer's instructions.

The V4 region of the bacterial 16S rRNA gene from the Earth Microbiome Project⁹⁵ were amplified using the updated primers 515 F GTGYCAGCMGCCGCGGTAA and 806 R GGACTACNVGGGTWTCTAAT with a single step and 25 cycles of polymerase chain reaction (PCR) using Phusion High-Fidelity PCR Kit (New England Biolabs Inc., Ipswich, MA). The following PCR profiles were used for amplifications: 96 °C for 2 min, and 25 cycles of 96 °C for 30 s, 55 °C for 30 s, 72 °C for 30 s and 72 °C for 5 min. All the amplicon products were purified using AMPure XP PCR (Beckman Coulter Inc., Beverly MA). All the samples were sequenced on the same Mi-seq Illumina sequencer run producing 2 \times 300 pb long reads. PCR and sequencing were conducted in the Molecular and Cellular Imaging Center of the Ohio State University (Wooster, USA). All sequences were deposited in GenBank under SRA accession number PRJNA893463.

Sequence analyses were performed with DADA2 (v1.22) using R software to analyze and correct Illumina sequence errors. The standard pipeline was applied with the following parameters trimLeft = 20, truncLen = c(220, 150), maxN = 0, maxEE = c(5,5), truncQ = 2. The sequences were filtered, dereplicated, and chimeras removed to obtain Amplicon Sequence Variants (ASVs). A total of 34,170 ASVs were obtained with a mean of 132,340 \pm 50,900 sequences for each ramet (Supplementary Table 13). ASVs were classified against the SILVA v.138.1 database for taxonomic assignment. ASVs representing algal contamination were removed. Two samples (one seawater and one coral sample from Fowey Rocks) were removed as they contained less than 10,000 reads.

Statistical analysis. All multivariate statistics on coral physiology and lipid class analyses were performed using the software Primer V6. To test the first hypothesis, coral physiological profiles (i.e., biomass, total lipids, total proteins, endosymbiont density, chlorophyll *a*, and $\delta^{13}\text{C}_{h-e}$) were compared among sites. Values from

duplicate ramets of the same genet were averaged prior to statistical analyses so that each genet was represented no more than once at each site, thus avoiding pseudoreplication. A Euclidian distance dissimilarity matrix was constructed from the normalized data. Since there were no coral genet effects (Supplementary Table 10), the parameter 'coral genet' was removed from the statistical models. $\delta^{15}\text{N}_{h-e}$ was not included in the model (Supplementary Fig. 6) as it is a co-variate with $\delta^{13}\text{C}_{h-e}$ ³². Differences in physiological profiles among sites were tested using a one-way analysis of similarity (ANOSIM, 9999 permutations) and visualized using a non-metric multidimensional scaling (nMDS) plot. The relative contribution of each physiological parameter to the sample distribution determined by Pearson's correlation analysis was visualized in the nMDS plots with vectors. The lipid class profiles (i.e., wax esters, triacylglycerol, sterols, acetone mobile polar lipids, and phospholipids) were similarly analyzed with the parameter coral genet removed from the model as there were no coral genet effects (Supplementary Table 11).

Univariate statistics were used to evaluate the effect of site on each physiological variable and lipid class individually. All univariate statistics were performed using the software R (V3.4.3). The distributions were normal ($p > 0.05$, Shapiro-Wilk tests) for the acetone-mobile polar lipids and the phospholipids allowing for multiple-factors ANOVA analysis. The remaining physiological parameters and lipid classes did not meet assumptions of normality ($p < 0.05$, Shapiro-Wilk tests). For the latter variables, multiple comparison non-parametric Kruskal-Wallis tests were used to test for differences among sites. All parameters did meet assumptions of homoscedasticity. Post-hoc Tukey tests were performed to determine which sites differed from each other for each physiological parameter and lipid class.

To test the second hypothesis concerning the coral microbiome, all bacterial sequences were normalized by dividing counts by sample size to obtain a relative abundance. The parameter 'coral genet' was removed from the models as there were no genet effects detected (Supplementary Table 12). Statistical tests among seawater bacterial communities were not performed because of small sample sizes. Possible differences of bacterial community composition were assessed by correspondence analysis (CA) with the phyloseq package in R⁹⁶ and significant differences among sites, corals, and combined seawater samples were tested using analysis of similarities (ANOSIM). The Bray-Curtis index and the Shannon diversity index were computed for all samples with the vegan package in R⁹⁷. Similarity percentage analysis (SIMPER) was performed with the vegan package to identify the ASVs that contributed proportionally the most to the differences observed among sites. Additional downstream univariate analyses were performed to compare relative abundance of the selected ASVs among sites. Finally, to determine if the physiology-based NMDS distribution pattern correlated to the microbial-based NMDS distribution pattern, we performed a Balance Evaluation Systems Test (BEST test).

Reporting summary. Further information on research design is available in the Nature Portfolio Reporting Summary linked to this article.

Data availability

All metadata and data that support the results of this study are available in U.S. Geological Survey data releases^{44,83,84}. Next-generation sequencing data are available in the NCBI Sequence Read Archive under accession number PRJNA893463.

Code availability

The code for the bioinformatics work on the microbiome are found in the DADA2 pipeline (<https://benjineb.github.io/dada2/tutorial.html>) and phyloseq package (<https://www.bioconductor.org/packages/release/bioc/html/phyloseq.html>).

Received: 15 November 2022; Accepted: 12 June 2023;

Published online: 17 July 2023

References

1. Aronson, R. B. & Precht, W. F. White-band disease and the changing face of Caribbean coral reefs. In: *The Ecology and Etiology of Newly Emerging Marine Diseases* (ed. Porter, J. W.) 25–38 (Springer Netherlands, 2001). https://doi.org/10.1007/978-94-017-3284-0_2
2. Bruckner, A. W. Proceedings of the Caribbean Acropora workshop: Potential application of the U.S. endangered species act as a conservation strategy. *NOAA Technical Memorandum NMFS-OPR-24*, Silver Spring, 199 (2002).
3. Aronson, R., Bruckner, A. W., Moore, J., Precht, B. & Weil. *Acropora palmata*. The IUCN red list of threatened species: e.T133381A3716457. 2008. Available at <https://doi.org/10.2305/IUCN.UK.2008.RLTS.T133381A3716457.en> (2008).
4. Miller, M., Bourque, A. & Bohnsack, J. An analysis of the loss of acroporid corals at Looe Key, Florida, USA: 1983–2000. *Coral Reefs* **21**, 179–182 (2002).
5. Hubbard, D. K. Controls of modern and fossil reef development common ground for biological and geological research. In: *Proceedings of the 6th*

- International Coral Reef Symposium: Vol. 1: Plenary Addressess and Status review.* 243–252 (1988).
6. Macintyre, I. G. & Glynn, P. W. Evolution of modern Caribbean fringing reef, Galeta Point, Panama. *Am. Assoc. Pet. Geol. Bull.* **60**, 1054–1072 (1976).
 7. Alvarez-Filip, L., Dulvy, N. K., Gill, J. A., Côté, I. M. & Watkinson, A. R. Flattening of Caribbean coral reefs: region-wide declines in architectural complexity. *Proc. R. Soc. B Biol. Sci.* **276**, 3019–3025 (2009).
 8. Costanza, R. et al. The value of the world's ecosystem services and natural capital. *Nature* **387**, 253–260 (1997).
 9. Spalding, M. et al. Mapping the global value and distribution of coral reef tourism. *Mar. Policy* **82**, 104–113 (2017).
 10. Gardner, T. A., Côté, I. M., Gill, J. A., Grant, A. & Watkinson, A. R. Hurricanes and Caribbean coral reefs: impacts, recovery patterns, and role in long-term decline. *Ecology* **86**, 174–184 (2005).
 11. Williams, D. E., Miller, M. W. & Kramer, K. L. Recruitment failure in Florida Keys *Acropora palmata*, a threatened Caribbean coral. *Coral Reefs* **27**, 697–705 (2008).
 12. Williams, D. E. & Miller, M. W. Attributing mortality among drivers of population decline in *Acropora palmata* in the Florida Keys (USA). *Coral Reefs* **31**, 369–382 (2012).
 13. Albright, R., Mason, B., Miller, M. & Langdon, C. Ocean acidification compromises recruitment success of the threatened Caribbean coral *Acropora palmata*. *Proc. Natl. Acad. Sci.* **107**, 20400–20404 (2010).
 14. Sutherland, K. P. et al. Shifting white pox aetiologies affecting *Acropora palmata* in the Florida Keys, 1994–2014. *Philos. Trans. R. Soc. B Biol. Sci.* **371**, 20150205 (2016).
 15. Kemp, K. M., Westrich, J. R., Alabady, M. S., Edwards, M. L. & Lipp, E. K. Abundance and multilocus sequence analysis of *Vibrio* bacteria associated with diseased elkhorn coral (*Acropora palmata*) of the Florida Keys. *Appl. Environ. Microbiol.* **84**, e01035–17 (2018).
 16. Baumann, J., Grottoli, A. G., Hughes, A. D. & Matsui, Y. Photoautotrophic and heterotrophic carbon in bleached and non-bleached coral lipid acquisition and storage. *J. Exp. Mar. Biol. Ecol.* **461**, 469–478 (2014).
 17. Anthony, K. R. N., Hoogenboom, M. O., Maynard, J. A., Grottoli, A. G. & Middlebrook, R. Energetics approach to predicting mortality risk from environmental stress: a case study of coral bleaching. *Funct. Ecol.* **23**, 539–550 (2009).
 18. Hughes, T. P., Graham, N. A. J., Jackson, J. B. C., Mumby, P. J. & Steneck, R. S. Rising to the challenge of sustaining coral reef resilience. *Trends Ecol. Evol.* **25**, 633–642 (2010).
 19. McLachlan, R. H., Dobson, K. L., Schmeltzer, E. R., Vega Thurber, R. & Grottoli, A. G. A review of coral bleaching specimen collection, preservation, and laboratory processing methods. *PeerJ* **9**, e11763 (2021).
 20. Grottoli, A. G., Rodrigues, L. J. & Palardy, J. E. Heterotrophic plasticity and resilience in bleached corals. *Nature* **440**, 1186–1189 (2006).
 21. Baums, I. B., Miller, M. W. & Hellberg, M. E. Geographic variation in clonal structure in a reef-building Caribbean coral, *Acropora palmata*. *Ecol. Monogr.* **76**, 503–519 (2006).
 22. Lirman, D. Fragmentation in the branching coral *Acropora palmata* (Lamarck): growth, survivorship, and reproduction of colonies and fragments. *J. Exp. Mar. Biol. Ecol.* **251**, 41–57 (2000).
 23. Kuffner, I. B., Stathakopoulos, A., Toth, L. T. & Bartlett, L. A. Reestablishing a stepping-stone population of the threatened elkhorn coral *Acropora palmata* to aid regional recovery. *Endanger. Species Res.* **43**, 461–473 (2020).
 24. Baums, I. B., Miller, M. W. & Hellberg, M. E. Regionally isolated populations of an imperiled Caribbean coral, *Acropora palmata*. *Mol. Ecol.* **14**, 1377–1390 (2005).
 25. Kourafalou, V. H., Androulidakis, Y. S., Kang, H., Smith, R. H. & Valle-Levinson, A. Physical connectivity between Pulley Ridge and Dry Tortugas coral reefs under the influence of the Loop Current/Florida Current system. *Prog. Oceanogr.* **165**, 75–99 (2018).
 26. Lee, T. N., Leaman, K., Williams, E., Berger, T. & Atkinson, L. Florida current meanders and gyre formation in the southern Straits of Florida. *J. Geophys. Res.* **100**, 8607–8620 (1995).
 27. Lee, T. N., Clarke, M. E., Williams, A. F., Szmant, A. M. & Berger, T. Evolution of the Tortugas Gyre and its influence on recruitment in the Florida Keys. *Bull. Mar. Sci.* **54**, 621–646 (1994).
 28. Hughes, A. D. & Grottoli, A. G. Heterotrophic compensation: a possible mechanism for resilience of coral reefs to global warming or a sign of prolonged stress? *PLoS ONE* **8**, e81172 (2013).
 29. Grottoli, A. G. et al. Coral physiology and microbiome dynamics under combined warming and ocean acidification. *PLOS ONE* **13**, e0191156 (2018).
 30. Krediet, C. J., Ritchie, K. B., Paul, V. J. & Teplitski, M. Coral-associated microorganisms and their roles in promoting coral health and thwarting diseases. *Proc. R. Soc. B Biol. Sci.* **280**, 20122328 (2013).
 31. Peixoto, R. S., Harkins, D. M. & Nelson, K. E. Advances in microbiome research for animal health. *Annu. Rev. Anim. Biosci.* **9**, 289–311 (2021).
 32. Price, J. T., McLachlan, R. H., Jury, C. P., Toonen, R. J. & Grottoli, A. G. Isotopic approaches to estimating the contribution of heterotrophic sources to Hawaiian corals. *Limnol. Oceanogr.* **66**, 2393–2407 (2021).
 33. Schoepf, V. et al. Annual coral bleaching and the long-term recovery capacity of coral. *Proc. R. Soc. B Biol. Sci.* **282**, 20151887 (2015).
 34. Rodrigues, L. J. & Grottoli, A. G. Calcification rate and the stable carbon, oxygen, and nitrogen isotopes in the skeleton, host tissue, and zooxanthellae of bleached and recovering Hawaiian corals. *Geochim. Cosmochim. Acta* **70**, 2781–2789 (2006).
 35. Rodrigues, L. J., Grottoli, A. G. & Pease, T. K. Lipid class composition of bleached and recovering *Porites compressa* Dana, 1846 and *Montipora capitata* Dana, 1846 corals from Hawaii. *J. Exp. Mar. Biol. Ecol.* **358**, 136–143 (2008).
 36. Solomon, S. L. et al. Lipid class composition of annually bleached Caribbean corals. *Mar. Biol.* **167**, 7 (2020).
 37. Conlan, J. A., Bay, L. K., Jones, A., Thompson, A. & Francis, D. S. Seasonal variation in the lipid profile of *Acropora millepora* at Halfway Island, Great Barrier Reef. *Coral Reefs* **39**, 1753–1765 (2020).
 38. Ermolenko, E. V. & Sikorskaya, T. V. Lipidome of the reef-building coral *Acropora cerealis*: changes under thermal stress. *Biochem. Syst. Ecol.* **97**, 104276 (2021).
 39. Reshef, L., Koren, O., Loya, Y., Zilber-Rosenberg, I. & Rosenberg, E. The coral probiotic hypothesis. *Environ. Microbiol.* **8**, 2068–2073 (2006).
 40. Rosenberg, E., Koren, O., Reshef, L., Efrony, R. & Zilber-Rosenberg, I. The role of microorganisms in coral health, disease and evolution. *Nat. Rev. Microbiol.* **5**, 355–362 (2007).
 41. Kuffner, I. B., Hickey, T. D. & Morrison, J. M. Calcification rates of the massive coral *Siderastrea siderea* and crustose coralline algae along the Florida Keys (USA) under-reef tract. *Coral Reefs* **32**, 987–997 (2013).
 42. Lenz, E. A., Bartlett, L. A., Stathakopoulos, A. & Kuffner, I. B. Physiological differences in bleaching response of the coral *Porites astreoides* along the Florida Keys reef tract during high-temperature stress. *Front. Mar. Sci.* **8**, 615795 (2021).
 43. Shaver, E. C. et al. A roadmap to integrating resilience into the practice of coral reef restoration. *Glob. Change Biol.* **28**, 4751–4764 (2022).
 44. Kuffner, I. B. Underwater temperature on off-shore coral reefs of the Florida Keys, U.S.A. (ver. 7.0. March 2022): U.S. Geological Survey data release. <https://doi.org/10.5066/F71C1TZK> (2016).
 45. Palardy, J., Grottoli, A. & Matthews, K. Effects of upwelling, depth, morphology and polyp size on feeding in three species of Panamanian corals. *Mar. Ecol. Prog. Ser.* **300**, 79–89 (2005).
 46. Zhu, W. et al. Consistent responses of coral microbiome to acute and chronic heat stress exposures. *Mar. Environ. Res.* **185**, 105900 (2023).
 47. Rosales, S. M. et al. Microbiome differences in disease-resistant vs. susceptible *Acropora* corals subjected to disease challenge assays. *Sci. Rep.* **9**, 18279 (2019).
 48. Naumann, M. S. et al. Organic matter release by dominant hermatypic corals of the Northern Red Sea. *Coral Reefs* **29**, 649–659 (2010).
 49. Wellington, G. M. An experimental analysis of the effects of light and zooplankton on coral zonation. *Oecologia* **52**, 311–320 (1982).
 50. Dobson, K. L., Ferrier-Pagès, C., Saup, C. M. & Grottoli, A. G. The effects of temperature, light, and feeding on the physiology of *Pocillopora damicornis*, *Stylophora pistillata*, and *Turbinaria reniformis* corals. *Water* **13**, 2048 (2021).
 51. Ferrier-Pagès, C., Witting, J., Tambutté, E. & Sebens, K. P. Effect of natural zooplankton feeding on the tissue and skeletal growth of the scleractinian coral *Stylophora pistillata*. *Coral Reefs* **22**, 229–240 (2003).
 52. Harriott, V. J. Coral lipids and environmental stress. *Environ. Monit. Assess.* **25**, 131–139 (1993).
 53. Teece, M. A., Estes, B., Gelsleichter, E. & Lirman, D. Heterotrophic and autotrophic assimilation of fatty acids by two scleractinian corals, *Montastraea faveolata* and *Porites astreoides*. *Limnol. Oceanogr.* **56**, 1285–1296 (2011).
 54. Towle, E. K., Enochs, I. C. & Langdon, C. Threatened Caribbean coral is able to mitigate the adverse effects of ocean acidification on calcification by increasing feeding rate. *PLoS ONE* **10**, e0123394 (2015).
 55. Grottoli, A. G. Effect of light and brine shrimp on skeletal $\delta^{13}\text{C}$ in the Hawaiian coral *Porites compressa*: a tank experiment. *Geochim. Cosmochim. Acta* **66**, 1955–1967 (2002).
 56. Bourne, D. G., Morrow, K. M. & Webster, N. S. Insights into the coral microbiome: underpinning the health and resilience of reef ecosystems. *Annu. Rev. Microbiol.* **70**, 317–340 (2016).
 57. Sunagawa, S. et al. Bacterial diversity and White Plague Disease-associated community changes in the Caribbean coral *Montastraea faveolata*. *ISME J* **3**, 512–521 (2009).
 58. Mhuantong, W. et al. Comparative analysis of bacterial communities associated with healthy and diseased corals in the Indonesian sea. *PeerJ* **7**, e8137 (2019).
 59. Closek, C. J. et al. Coral transcriptome and bacterial community profiles reveal distinct Yellow Band disease states in *Orbicella faveolata*. *ISME J* **8**, 2411–2422 (2014).
 60. Chu, N. D. & Vollmer, S. V. Caribbean corals house shared and host-specific microbial symbionts over time and space. *Environ. Microbiol. Rep.* **8**, 493–500 (2016).

61. Kemp, D. W. et al. Spatial homogeneity of bacterial communities associated with the surface mucus layer of the reef-building coral *Acropora palmata*. *PLoS ONE* **10**, e0143790 (2015).
62. Liburn, T. G. et al. Nitrogen fixation by symbiotic and free-living. *Spirochetes. Sci.* **292**, 2495–2498 (2001).
63. Qin, Z. et al. Microbiome of juvenile corals in the outer reef slope and lagoon of the South China Sea: insight into coral acclimatization to extreme thermal environments. *Environ. Microbiol.* **23**, 4389–4404 (2021).
64. Bakkiyaraj, D., Sivasankar, C. & Pandian, S. K. Anti-pathogenic potential of coral associated bacteria isolated from Gulf of Mannar against *Pseudomonas aeruginosa*. *Indian J. Microbiol.* **53**, 111–113 (2013).
65. Spring, S., Scheuner, C., Göker, M. & Klenk, H.-P. A taxonomic framework for emerging groups of ecologically important marine gammaproteobacteria based on the reconstruction of evolutionary relationships using genome-scale data. *Front. Microbiol.* **6**, 281 (2015).
66. Yang, S.-Y. et al. Effects of ocean acidification on coral endolithic bacterial communities in *Isopora palifera* and *Porites lobata*. *Front. Mar. Sci.* **7**, 603293 (2020).
67. Palardy, J. E., Grottoli, A. G. & Matthews, K. A. Effect of naturally changing zooplankton concentrations on feeding rates of two coral species in the Eastern Pacific. *J. Exp. Mar. Biol. Ecol.* **331**, 99–107 (2006).
68. Heidelberg, K. B., Sebens, K. P. & Purcell, J. E. Composition and sources of near reef zooplankton on a Jamaican forereef along with implications for coral feeding. *Coral Reefs* **23**, 263–276 (2004).
69. Levas, S. et al. Can heterotrophic uptake of dissolved organic carbon and zooplankton mitigate carbon budget deficits in annually bleached corals? *Coral Reefs* **35**, 495–506 (2016).
70. Kourafalou, V. H. & Kang, H. Florida Current meandering and evolution of cyclonic eddies along the Florida keys reef tract: are they interconnected?: Florida current and cyclonic eddies. *J. Geophys. Res. Oceans* **117**, C05028 (2012).
71. Sawall, Y., Harris, M., Lebrato, M., Wall, M. & Feng, E. Y. Discrete pulses of cooler deep water can decelerate coral bleaching during thermal stress: implications for artificial upwelling during heat stress events. *Front. Mar. Sci.* **7**, 720 (2020).
72. Weisberg, R. H. & He, R. Local and deep-ocean forcing contributions to anomalous water properties on the West Florida Shelf. *J. Geophys. Res. Oceans* **108**, 3184 (2003).
73. Sponaugle, S. et al. Near-reef zooplankton differs across depths in a subtropical seascape. *J. Plankton Res.* **43**, 586–597 (2021).
74. Riegl, B. et al. Heat attenuation and nutrient delivery by localized upwelling avoided coral bleaching mortality in northern Galapagos during 2015/2016 ENSO. *Coral Reefs* **38**, 773–785 (2019).
75. Chen, Y.-H., Shertzer, K. W. & Viehman, T. S. Spatio-temporal dynamics of the threatened elkhorn coral *Acropora palmata*: Implications for conservation. *Divers. Distrib.* **26**, 1582–1597 (2020).
76. Szmant, A. M. & Forrester, A. Water column and sediment nitrogen and phosphorus distribution patterns in the Florida Keys, USA. *Coral Reefs* **15**, 21–41 (1996).
77. Briceño, H. O. & Boyer, J. N. 2020 annual report of the water quality monitoring project for the Florida Keys National Marine Sanctuary. <http://serc.fiu.edu/wqmnetwork/Reports/FKNMS/2020%20FKNMS%20Annual%20Report.pdf> (2021).
78. Boyer, J. N. & Briceño, H. O. Southeast environmental research center Florida International University Miami, FL 33199 <http://serc.fiu.edu/wqmnetwork/> (2006).
79. Cunning, R. et al. Census of heat tolerance among Florida's threatened staghorn corals finds resilient individuals throughout existing nursery populations. *Proc. R. Soc. B Biol. Sci.* **288**, 20211613 (2021).
80. Lirman, D. et al. Growth dynamics of the threatened Caribbean staghorn coral *Acropora cervicornis*: influence of host genotype, symbiont identity, colony size, and environmental setting. *PLoS ONE* **9**, e107253 (2014).
81. Drury, C., Manzello, D. & Lirman, D. Genotype and local environment dynamically influence growth, disturbance response and survivorship in the threatened coral, *Acropora cervicornis*. *PLoS ONE* **12**, e0174000 (2017).
82. Neely, K. L., Macaulay, K. A. & Lunz, K. S. Population trajectory and stressors of *Acropora palmata* sites in the Florida Keys. *Front. Mar. Sci.* **9**, 978785 (2022).
83. Kuffner, I. B., Stathakopoulos, A., Toth, L. T. & Bartlett, L. A. Experimental coral-growth rates and time-series imagery data for *Acropora palmata* in the Florida Keys, U.S.A.: U.S. Geological Survey data release <https://doi.org/10.5066/P9KZEGXY> (2020).
84. Chapron, L. et al. Experimental coral-physiology data for *Acropora palmata* in Florida, U.S.A.: U.S. Geological Survey data release <https://doi.org/10.5066/P9FIBAKX> (2023).
85. NOAA National Centers for Environmental Information. *National Data Buoy Center. Meteorological and oceanographic data collected from the National Data Buoy Center Coastal-Marine Automated Network (C-MAN) and moored (weather) buoys.* <https://www.ncei.noaa.gov/archive/accession/NDBC-CMANWx> (1971).
86. Marsh, J. A. Primary productivity of reef-building calcareous red algae. *Ecology* **51**, 255–263 (1970).
87. Mclachlan, R., Dobson, K. & Grottoli, G. A. Quantification of total biomass in ground coral samples. *protocols.io*, <https://doi.org/10.17504/protocols.io.bdyai7se> (2020).
88. Mclachlan, R., Juracka, C. & Grottoli, G. A. Symbiodiniaceae enumeration in ground coral samples using Countess™ II fl automated cell counter. *protocols.io*, <https://doi.org/10.17504/protocols.io.bdc5i2y6> (2020).
89. Jeffrey, S. T. & Humphrey, G. F. New spectrophotometric equations for determining chlorophylls a, b, c1 and c2 in higher plants, algae and natural phytoplankton. *Biochem. Physiol. Pflanz.* **167**, 191–194 (1975).
90. Mclachlan, R., Munoz-Garcia, A. & Grottoli, G. A. Extraction of total soluble lipid from ground coral samples. *protocols.io* <https://doi.org/10.17504/protocols.io.bc4qiyvw> (2020).
91. Bradford, M. M. A rapid and sensitive method for the quantitation of microgram quantities of protein utilizing the principle of protein-dye binding. *Anal. Biochem.* **72**, 248–254 (1976).
92. Gnaiger, E. & Bitterlich, G. Proximate biochemical composition and calorific content calculated from elemental CHN analysis: a stoichiometric concept. *Oecologia* **62**, 289–298 (1984).
93. Muscatine, L. & Porter, J. W. Reef corals: Mutualistic symbioses adapted to nutrient-poor environments. *BioScience* **27**, 454–460 (1977).
94. Keister, E. F., Gantt, S. E., Reich, H. G. et al. Similarities in biomass and energy reserves among coral colonies from contrasting reef environments. *Sci. Rep.* **13**, 1355 (2023).
95. Caporaso, J. G. et al. Global patterns of 16S rRNA diversity at a depth of millions of sequences per sample. *Proc. Natl. Acad. Sci.* **108**, 4516–4522 (2011).
96. McMurdie, P. J. & Holmes, S. phyloseq: An R package for reproducible interactive analysis and graphics of microbiome census data. *PLoS ONE* **8**, e61217 (2013).
97. Oksanen, J. et al. Package ‘vegan’. *Community Ecol. Package Version* **29**, 1–295 (2013).

Acknowledgements

The funding for this work was provided by the U.S. Geological Survey, Coastal and Marine Hazards and Resources Program, including agreement number G19AC00418 to AGG at The Ohio State University, and the National Science Foundation (OCE 1838667) to AGG. We thank Matthew Sullivan for his generous logistical support, B. J. Reynolds for his contribution in the field, and Captain Joe Bailey for assistance on board the M/V Makai. The study was conducted under scientific research permits from the Florida Keys National Marine Sanctuary (FKNMS-2016-085-A1 and FKNMS-2019-139) and the National Park Service (BISC-2018-SCI-0014, BISC-2019-SCI-0010, DRTO-2017-SCI-0001, and DRTO-2019-SCI-0005). Any use of trade, firm, or product names is for descriptive purposes only and does not imply endorsement by the U.S. Government. We also thank Lisa Rodrigues, Alexis Sturm, and two anonymous reviewers for providing helpful comments on the manuscript.

Author contributions

L.C., I.B.K., and A.G.G. designed the study. L.C., I.B.K., A.M.H., A.S., E.O.L., and A.G.G., participated in the fieldwork. D.W.K. and E.F.K. trained L.C. for the lipid class analysis. L.C. carried out laboratory and data analyses and wrote the first draft of the manuscript. L.C., I.B.K., D.W.K., A.M.H., E.F.K., A.S., L.A.B., E.O.L., and A.G.G. contributed to revising the manuscript.

Competing interests

The authors declare no competing interests.

Additional information

Supplementary information The online version contains supplementary material available at <https://doi.org/10.1038/s43247-023-00888-1>.

Correspondence and requests for materials should be addressed to Leila Chapron or Andréa G. Grottoli.

Peer review information *Communications Earth & Environment* thanks Alex Sturm, Julie Meyer and the other, anonymous, reviewer(s) for their contribution to the peer review of this work. Primary Handling Editors: Christopher Cornwall, Clare Davis, Heike Langenberg.

Reprints and permission information is available at <http://www.nature.com/reprints>

Publisher's note Springer Nature remains neutral with regard to jurisdictional claims in published maps and institutional affiliations.



Open Access This article is licensed under a Creative Commons Attribution 4.0 International License, which permits use, sharing, adaptation, distribution and reproduction in any medium or format, as long as you give appropriate credit to the original author(s) and the source, provide a link to the Creative Commons license, and indicate if changes were made. The images or other third party material in this article are included in the article's Creative Commons license, unless indicated otherwise in a credit line to the material. If material is not included in the article's Creative Commons license and your intended use is not permitted by statutory regulation or exceeds the permitted use, you will need to obtain permission directly from the copyright holder. To view a copy of this license, visit <http://creativecommons.org/licenses/by/4.0/>.

© The Author(s) 2023